Biometrical Journal

WILEY-VCH

Biometrical Journal

RESEARCH ARTICLE OPEN ACCESS

Wavelet-Mixed Landmark Survival Models for the Effect of Short-Term Changes of Potassium in Heart Failure Patients

Caterina Gregorio[1,2,3] | Giulia Barbati[2] | Arjuna Scagnetto[4] | Andrea di Lenarda[4] | Francesca Ieva[1,5]

[1]MOX - Modelling and Scientific Computing, Department of Mathematics Politecnico di Milan, Milan, Italy | [2]Biostatistics Unit, Department of Medical Sciences, University of Trieste, Trieste, Italy | [3]Aging Research Center, Department of Neurobiology, Care Sciences and Society, Karolinska Institutet and Stockholm University, Stockholm, Sweden | [4]Territorial Specialistic Department, University Hospital and Health Services of Trieste, Trieste, Italy | [5]HDS, Health Data Science Center, Human Technopole, Milan, Italy

Correspondence: Caterina Gregorio (caterina.gregorio@ki.se)

Received: 28 November 2023 | **Revised:** 15 September 2024 | **Accepted:** 22 September 2024

Funding: This work was supported by VIFOR Pharma.

Keywords: biomarker monitoring | dynamic survival models | electronic health records | heart failure

ABSTRACT

Statistical methods to study the association between a longitudinal biomarker and the risk of death are very relevant for the long-term care of subjects affected by chronic illnesses, such as potassium in heart failure patients. Particularly in the presence of comorbidities or pharmacological treatments, sudden crises can cause potassium to undergo very abrupt yet transient changes. In the context of the monitoring of potassium, there is a need for a dynamic model that can be used in clinical practice to assess the risk of death related to an observed patient's potassium trajectory. We considered different landmark survival approaches, starting from the simple approach considering the most recent measurement. We then propose a novel method based on wavelet filtering and landmarking to retrieve the prognostic role of past short-term potassium shifts. We argue that while taking into account the smooth changes in the biomarker, short-term changes cannot be overlooked. State-of-the-art dynamic survival models are prone to give more importance to the smooth component of the potassium profiles. However, our findings suggest that it is essential to also take into account recent potassium instability to capture all the relevant prognostic information. The data used comes from over 2000 subjects, with a total of over 80,000 repeated potassium measurements collected through administrative health records. The proposed wavelet landmark method revealed the prognostic role of past short-term changes in potassium. We also performed a simulation study to assess how and when to apply the proposed wavelet-mixed landmark model.

1 | Introduction

In recent years, medical research has increasingly relied on the integration of administrative and electronic health recording systems, providing vast amounts of longitudinal data from real-world contexts. Such data are crucial in extracting real-world evidence that can help manage complex conditions, such as heart failure.

Heart failure is a consequence of many cardiovascular diseases. However, despite improvements in treatments, mortality, and hospitalization rates remain high in heart failure disease. Monitoring patients' disease progression and status over time using easily measurable biomarkers, such as potassium, is crucial for making medical decisions regarding treatments. Potassium alterations are common in heart failure patients due to the disease itself, pharmacological treatment, and comorbidities.

This is an open access article under the terms of the Creative Commons Attribution-NonCommercial-NoDerivs License, which permits use and distribution in any medium, provided the original work is properly cited, the use is non-commercial and no modifications or adaptations are made.

© 2025 The Author(s). *Biometrical Journal* published by Wiley-VCH GmbH.

Dyskalemia, or potassium disorders, can lead to life-threatening conditions, with both low (hypokalemia) and high (hyperkalemia) levels being dangerous. Clinical guidelines set the normal range of serum potassium between 3.5 and 5.0 mmol/L in the general population. However, recent studies have raised serious concerns about the validity of this range in patients affected by heart failure (Cooper et al. 2020; Ferreira et al. 2020). This work has been motivated by the need to further study the role of potassium dynamics and to provide a tool for the monitoring of potassium in the health care of heart failure patients. However, potassium in heart failure patients is characterized by sudden but typically transient changes, making it challenging to study its temporal evolution. Since the final goal of medical decisions is the minimization of the risk of adverse events such as hospitalizations or death, dynamic survival models can be used to build prognostic clinical models to study the association between time-to-event outcomes and biomarkers over time. In this article, we consider different landmark survival models with potassium as the biomarker of interest using electronic health records data. This class of models allows taking into account that the value of biomarker changes over time and with that, the risk of adverse events needs to be updated. The most simple approach to dynamic predictions is the standard landmarking (van Houwelingen and Putter 2011). This approach resembles what is most typically done in clinical practice. Only the most recent measurement of the biomarker is taken into account. Moreover, the assessment of such values is done mainly through cutoffs which distinguish "normal" values from "abnormal" ones. The major drawback of this method is that past information given by repeated measurements is either not considered in the medical assessment or used qualitatively. On the other hand, it has been shown that exploiting all available information and quantitatively assessing the risk of an individual biomarker trajectory observed up to a time can be much more informative. In the last few years, most of the literature involving dynamic survival models has been based on more advanced approaches based on landmarking, such as the landmarking coupled with linear mixed effect models (Ferrer et al. 2019; Rizopoulos et al. 2017). This work aims to explore the advantages and limitations of current landmark methods used to analyze the relationship between potassium dynamics and time-to-event outcomes taking into account its peculiar behavior that exhibits sudden short-term changes. For this reason, a new approach using wavelets is proposed to better understand the role of how local variations in potassium levels may affect mortality risk depending on the time and their duration. Wavelet filters are common methods in time series analysis (Nason and Von Sachs 1999) and signal processing (Unser and Aldroubi 1996) to extract relevant features from data and remove noise. One of their characteristics is their ability to identify changes that occur at different frequencies. We believe that this can also be an insightful feature in the context of clinical monitoring of biomarkers such as potassium. In Section 2, we describe the data used in this article. Section 3 describes the statistical methods. First, the concept of dynamic predictions is presented, and then the different methods considered in this article to obtain dynamic predictions are introduced: the landmark last observation carried forward (LOCF) model (Section 3.2), the landmark mixed survival model (Section 3.3), and finally the novel landmark wavelet model (Section 3.4). An extensive simulation study was performed to evaluate the appropriateness of applying the proposed wavelet method to longitudinal potassium data and in the context of dynamic survival modeling problems (Section 4). The results of the real-world data application are given in Section 5. In Section 5.1, a general description of the cohort is given, while in Section 5.2 potassium repeated measurement data are described. The results of the different landmark survival models are shown in Section 5.3. The performance and comparison of the different approaches in terms of goodness-of-fit and dynamic predictive accuracy in the application under study are reported in Section 5.4. Finally, the discussion and conclusions are in Section 6.

2 | Study Design and Data

Data were obtained by the interrogation of the administrative regional health data of Friuli Venezia Giulia Region in the Northern part of Italy, integrated with data derived from the Outpatient and Inpatient Clinic E-chart (Cardionet). This integrated database constitutes the Trieste Observatory of Cardiovascular Diseases. Specifically, this was a cohort observational, noninterventional study involving patients living in the Trieste area who had a heart failure diagnosis between January 2009 and December 2020, had at least one cardiological evaluation, and two potassium measurements, and were observed for at least 1 year. For the identification of the heart failure patients, the following steps were followed. First, a search in the electronic medical records, using appropriate keywords (heart failure, chronic heart failure, systolic heart failure, diastolic heart failure) to select patients with heart failure–related clinical findings. In order to avoid any diagnostic underestimation, data from the medical E-chart were combined with the discharge codes of any previous hospital access (based on the standard nomenclature of the ICD-9 CM) and/or interventional procedures for heart failure patients (i.e., ICD implantation). Subsequently, prospective cases were manually reviewed by clinicians to validate the diagnosis of heart failure using the criteria established in 2016 by the European Cardiology Society. The cohort was followed from the index date, defined as the date of the first ambulatory visit with a potassium measure available, until the time of death or the end of the follow-up (administrative study closure date, fixed at December 31, 2020). The database has been previously described in the literature (Iorio et al. 2019). For this specific study, demographic, clinical, and instrumental variables at the index date together with all repeated blood tests containing the potassium measurements have been considered.

3 | Methods

Let $\mathcal{D}_n = \{Z_i, \delta_i, \mathbf{y}_i; i = 1, \dots, n\}$ denote a sample from the target population, where T_i and C_i are the individual's death and censoring time, respectively. We assume that C_i is noninformative with respect to the potassium process and death time. For each patient, we only observe the couple $Z_i = \min(T_i, C_i)$, $\delta_i = \mathbb{1}(T_i \leq C_i)$. Moreover, for each patient $i \in \{1, \dots, n\}$, we let $\mathbf{y}_i$ be the vector of longitudinal potassium measurements and y_{ij} a single measurement observed for the subject i at time t_{ij}, $j = 1, \dots, m_i$.

3.1 | Dynamic Predictions

The main objective is to provide a tool to extract from potassium longitudinal data observed up to a time, for example, in correspondence of a clinical visit of patients affected by heart failure, a quantitative assessment of patients' future risk of death. Using dynamic survival models, it is possible to derive individualized dynamic predictions of survival. We let k be the subject that has provided a set of longitudinal potassium measurements up to time t, $\mathcal{Y}_k(t) = \{y_k(t_{kj}); 0 \le t_{kj} \le t, j = 1, \dots, m_k\}$. The individual dynamic prediction is defined for a specified time horizon $w > t$ as the probability that the subject k will survive, at least up to w:

$$\pi_k(w|t) = Pr(T_k \ge w | T_k > t, \mathcal{Y}_k(t), \mathcal{D}_n). \quad (1)$$

Note that this is a conditional subject-specific prediction since the subject has survived to time t. The prediction is called dynamic in time because we can update it to get $\pi_k(w|t')$ as new information is collected at $t' > t$.

In the following sections, we describe different landmark methods to consider to obtain dynamic predictions of survival based on past potassium measurements. For each of them, different association structures between the longitudinal process and the landmark survival are also considered.

3.2 | Landmark LOCF

The standard conditional approach is one more similar to what is currently done in clinical practice. We can set a grid of time points, called landmarks, in which information on potassium can be updated. At each landmark point, we can study the association between potassium and time of death by estimating a Cox proportional hazard model using as a covariate the last potassium measurement collected before the landmark point. The dataset used for the estimation contains only patients still under observation at the landmark time. Moreover, only the events up to the fixed time horizon w are retained, while patients experiencing the event after the horizon are censored at the horizon time. Let $h = \{h_1, \dots, t, \dots, h_l\}$ the landmark times. To gain efficiency and interpretability, instead of estimating different models for each landmark time, we can specify a so-called "landmark supermodel" (van Houwelingen and Putter 2011):

$$h_i(l|\mathbf{z}_i, y_{ih}, h, w) = h_{h,0}(t) \exp\{\mathbf{z}_i\boldsymbol{\beta} + f(y_{ih})\gamma\}, h \le l \le h + w,$$

where $\mathbf{z}_i$ is the vector of a fixed covariate, $f(y_{ih})$ is a generic transformation of the last potassium assessment before time h and $\boldsymbol{\beta}$ and $\boldsymbol{\gamma}$ are the respective coefficients. Specifically, two different models with two alternative transformations of the last potassium measurements are considered. The first (LOCF a) considers the last observed measurement of potassium as a continuous value. Since both low and high values of potassium are believed to be dangerous, the last potassium measurement is allowed to have a nonlinear effect on the hazard through a cubic B-spline with 4 degrees of freedom (internal knots were placed at 25th, 50th, and 75th percentiles of the distribution). In the second model (LOCF b), from the last measurement of potassium, a categorical variable is derived using the cutoffs currently employed in the clinical practice. Specifically, potassium is considered "high" if greater than 5 mmol/L, "low" if below 3.5 mmol/L and, in the normal range otherwise. The dataset used for the estimation is the one made by stacking all the datasets used for the separate landmark models. It is important to note that an event can appear in the "stacked" dataset more than once if it falls in the $h + w$ interval for more than a landmark point h. This is the reason why the robust sandwich estimator for the standard errors is used.

Once the model has been estimated, an estimate of $\pi_k(w|t)$ for a subject k is obtained as

$$\hat{\pi}_k^{LOCF}(w|t) = \exp[-\hat{H}_{t,0}(w) \exp\{\mathbf{z}_k\hat{\boldsymbol{\beta}} + f(y_{kt})\hat{\gamma}\}],$$

where $\hat{H}_{t,0}(u)$ is the cumulative baseline hazard obtained using the Breslow estimator.

3.3 | Mixed Landmark Models

The LOCF landmark approach is relatively simple. However, it does not take into account any past information besides the last measurement or the fact that potassium, as any biomarker, is measured with error. To overcome these limitations, an extension to the previous model consists of modeling the individual potassium trajectories using a linear mixed effect model:

$$y_{it} = m_{it} + \epsilon_i(t) = (\boldsymbol{\alpha} + \mathbf{a}_i)f(t) + \tilde{\mathbf{x}}_i\tilde{\boldsymbol{\alpha}} + \epsilon_i(t), \quad (2)$$

where $\epsilon_i(t)$ is the Gaussian measurement error term with mean 0 and variance σ^2_ϵ, $f(\cdot)$ is a nonlinear function of time, $\boldsymbol{\alpha}$ and $\tilde{\boldsymbol{\alpha}}$ are fixed-effect coefficients for time and baseline covariates, respectively, and $\mathbf{a} \sim N(\mathbf{0}, \mathbf{D})$ are the random effects coefficients. A flexible dependence between the overall mean trajectory and time is defined through a natural cubic spline with d degrees of freedom (denoted in the following with $ns(\cdot)$). Subject-specific changes in the potassium trajectory can be determined by disease progression as well as drug intake, hospitalizations, and worsening of renal function. These are unobserved longitudinal processes, and their effect on potassium can be taken into account using time-related random effects. For the random effects, we consider a spline transform of time with the same degrees of freedom used for the fixed effects, to allow for the estimated individual potassium trajectories to be as flexible as possible.

In the landmark model, we can assume different association structures depending on how the risk of death is assumed to depend on potassium. A common choice is also that the hazard of death depends on the estimated value of the mean subject-specific trajectory at each of the landmark times and the slope of the potassium trajectory up to the landmark point (Rizopoulos et al. 2017):

$$\begin{aligned} &h_i(l|\mathbf{z}_i, y_{i0}, \dots, y_{ih}, h, w) \\ &\quad = h_{h,0}(t) \exp\{\mathbf{z}_i\boldsymbol{\beta} + f(\hat{m}_{ih})\boldsymbol{\gamma}_1 + \hat{m}'_{ih}\gamma_2\}, h \le l \le h + w, \end{aligned} \quad (3)$$

where $\hat{m}_{ih}$ can be predicted at the different landmark times by deriving the empirical Bayes estimates of the random effects and the estimated fixed effects from the linear mixed model in Equation (2) and $\hat{m}'_{ih}$ is the first derivative of $\hat{m}_{ih}$. As in the previous model, a cubic spline was used, as $f(\cdot)$ to allow $\hat{m}_{ih}$ to

have a nonlinear effect on the hazard of death. We will denote this model by a mixed model (MM).

In the same way as before, we can derive $\hat{m}_{kt}$ at time t for the subject k for whom we want to calculate the dynamic prediction based on measurements collected up to t. Therefore, similarly to the LOCF landmark approach, the dynamic predictions are obtained as

$$\hat{\pi}_k^{MIXED}(w|t) = \exp[-\hat{H}_{t,0}(w)\exp\{\mathbf{z}_k\hat{\boldsymbol{\beta}} + f(\hat{m}_{kt})\hat{\gamma}_1 + \hat{m}'_{kt}\hat{\gamma}_2\}]. \quad (4)$$

3.4 | Mixed-Wavelet Landmark Models

The approaches that use the linear mixed effects model to extract information from potassium measurements place a lot of emphasis on the slow and stable changes. They tend to treat transient changes as measurement errors to be forgotten. Therefore, both joint and mixed landmark models implicitly assume that past short-term changes in potassium do not affect the risk of adverse events. However, in patients with heart failure, past changes in potassium that are not reflected in the smooth component of the individual potassium profiles may be important to consider when monitoring potassium. To assess whether short-term changes play a role in shaping the risk of death, we propose a novel method based on landmarking and the wavelet Morlet (WM) filter (Carmona et al. 1998). In general, Morlet wavelets are continuous, complex-valued functions used to smooth nonstationary time-series data, and they allow for distinguishing the frequencies at which oscillations occur. The Morlet wavelet transform is characterized by a "mother wavelet": $\Psi(t) = \pi^{-1/4}e^{6it}e^{-t^2/2}$. In the application to dynamic survival models and potassium monitoring, we propose the use of the Morlet filter to extract from the repeated measurements' data, the times at which relevant changes happen. To achieve this, the data need to be de-trended so the Morlet transform is applied to the residuals of the linear mixed effect model specified in Equation (2), denoted by $\tilde{y}_{it}$. The set of frequencies which will determine the duration of the short-term changes that are allowed to be captured by the filtering also needs to be chosen. Here, we define equivalently their reciprocal, the periods (or duration) p. The short-term oscillation in potassium at time t and of duration within $p_1 \le p \le p_2$ is obtained using the Morlet wavelet transform as (Rösch et al. 2018):

$$\hat{s}_i^{p_1-p_2}(\tau) = \frac{df\,dt^{1/2}}{0.776\Phi(0)} \sum_{p=p_1,\dots,p_2} \hat{\theta}_i^{\tau,p} \frac{Re[Wave_i(\tau,p)]}{(1/p)^{1/2}},$$

where $Wave_i(\tau,p) = \sum_t \tilde{y}_i(t)\frac{1}{1/\sqrt{p}}\Psi^*\left(\frac{t-\tau}{1/p}\right)$, Ψ^* indicates the complex conjugate of Ψ. τ determines the position of a specific daughter wavelet in time, and df and dt are the frequency and time resolutions chosen. In our study, we set dt to 1 day and df to 1/2, aiming to detect short-term changes as brief as 2 days. Choosing 1 day as dt is reasonable when studying individual survival, as it reflects the desired level of detail in measuring follow-up time—a decision applicable to any event model. As for df, it can be easily determined by examining the data and considering the problem context. For instance, identifying the smallest interval between two measurement times can help inform the choice of df as it is the minimum duration of a short-term oscillation that can be observed in the biomarker. Finally, $Re(\cdot)$ denotes the real part. The filtering itself is carried out by the term $\hat{\theta}_i^{\tau,p}$, which is an indicator that retains only wavelets transform whose "strength" is not consistent with a white noise process. In the wavelet setting, "strength" is defined by the power spectrum. The latter is defined at a particular time and period as the square of the local amplitude of the corresponding wavelet transform component: $P_i(\tau,p) = p|Wave_i(\tau,p)|^2$, where $|\cdot|$ stands for the modulus. It is important to note that if no relevant oscillations are detected for some subjects at a duration interval of interest, $\hat{s}_i^{p_1-p_2}(\tau) \equiv 0$.

The duration windows of interest for potassium chosen were 2–14 days, 15–30 days, 31–90 days, 91–180 days, and 181–365 days. The rationale behind the choice of the intervals was the clinical interpretation of the short-term components. These intervals were discussed with the clinical experts involved in the study, and they reflect clinical practice routines. More specifically, potassium measurements are usually repeated within 14 days and again after 30 days during up-titration of the pharmacological treatments or more frequently when patients are hospitalized. In both cases, these can be considered possible reasons for the "acute crisis" in the values of potassium. On the other hand, 90, 180, and 365 days are the intervals where patients can be reevaluated by cardiologists and when effects of disease progression or worsening of comorbidities (e.g., chronic kidney disease [CKD]) on potassium can be observed.

Now in the landmark model, we assume that the risk of death does not only depend on the value of the mean subject-specific trajectory of the biomarker estimated through the linear mixed model as in the landmark mixed model but also on the short-term changes estimated at landmark times using the Morlet wavelet filter described above. Specifically, the landmark wavelet Cox model is now specified as

$$h_i(l|\mathbf{z}_i, y_{i0}, \dots, y_{ih}, h, w) = h_{h,0}(l)\exp\{\mathbf{z}_i\boldsymbol{\beta} + f_1(\hat{m}_{ih})\boldsymbol{\gamma}_1 + f_2(\hat{\mathbf{s}}_{ih})\boldsymbol{\theta}\}, h \le l \le h+w, \quad (5)$$

where $\mathbf{s}_{ih}$ is the vector of local changes in the biomarker at different duration intervals of interest for the subject i, $f_1(\cdot)$ is the nonlinear transform used for the term $\hat{m}_{ih}$ and $f_2(\cdot)$ considered for $\hat{\mathbf{s}}_{ih}$. As $f_1(\cdot)$, the same function as the one for the model in Equation (3) is used. In this case, two alternative models were considered: one with the cubic-spline transformation function as $f_2(\cdot)$, and the other with a categorical version defined as follows:

$$\hat{o}_i(h)^{p_1-p_2} = \begin{cases} "upward" & \text{if } \hat{s}_i(h)^{p_1-p_2} > 0 \\ "downward" & \text{if } \hat{s}_i(h)^{p_1-p_2} < 0 \\ "no" & \text{if } \hat{s}_i(h)^{p_1-p_2} = 0. \end{cases}$$

Note that it may also be of interest to consider a simpler model with only one short-term component with all durations between 2 and 365 days. In the following, we will start from this model (MW a). In addition, also the vector with continuous and categorical versions of the short-term changes in the different duration intervals will be considered. We will denote these models by MW b and MW c, respectively.

As in the previous landmark models, the dynamic prediction follows for subject k from the fitted Cox model as

$$\hat{\pi}_k^{WAVE}(w|t) = \exp[-\hat{H}_{t,0}(w)\exp\{\mathbf{z}_k\hat{\boldsymbol{\beta}} + f_1(\hat{m}_{kt})\hat{\boldsymbol{\gamma}}_1 + f_2(\hat{\mathbf{s}}_{kt})\hat{\boldsymbol{\theta}}\}]. \quad (6)$$

4 | Simulation Study

In the previous section, we discussed dynamic survival models that leverage information from repeated measures of potassium. We conducted a simulation study with two parts. The first part regards the longitudinal potassium trajectories only, while the second also considers the survival process.

4.1 | Longitudinal Potassium Process

Aims. The predictive accuracy of the landmark survival models heavily relies on the chosen method employed to obtain the individuals' biomarker trajectories. We have proposed the utilization of the wavelet filter, which is commonly employed in the medical signal and time-series domain. By combining the well-established linear mixed model with the wavelet filter, we propose a novel methodology for representing biomarker data with irregular intervals between measurements. Therefore, we aimed to assess the predictive accuracy in retrieving the potassium trajectories and the impact of various longitudinal model configurations on the accuracy and flexibility of capturing the underlying patterns in the potassium trajectories. The three subaims of this part of the simulation study were as follows: (1) Does the proposed WM filter adapted to improve the predictive accuracy of the longitudinal trajectories by capturing both high-frequency and low-frequency components of the potassium trajectory using biomarker data obtained from electronic health records with irregular measurement interval? (2) How do the degrees of freedom in the spline transformation of time affect the mixed model? What happens when the longitudinal model is misspecified, either with respect to the choice of the degrees of freedom for the spline transformation or the use of the WM filter?

Data-generating mechanism. To generate the potassium repeated measurement data, two different scenarios are considered. Under *Scenario 1*, to simulate realistic data, potassium longitudinal values are sampled with replacement from the real-world dataset (Morris et al. 2019). Such a simulation technique will help identify the best model without any idea of the true model. On the other hand, in *Scenario 2* the longitudinal potassium profiles are generated using a linear mixed-effect model similar to the one in Equation (2) with a spline transformation of time with 5 degrees of freedom. Therefore, in this second scenario, the biomarker profiles have a smooth behavior with no sudden changes. We generated 100 datasets, each containing the potassium trajectories of 1000 individuals. To ensure the synthetic data closely resembled the observed data in terms of heterogeneity and irregularities of the measurement times, in both scenarios, we sampled the measurement times with replacement from the real dataset. Additionally, the maximum follow-up time for each individual was sampled from a Weibull distribution with a scale parameter equal to 3083 and a shape parameter of 1.80.

Estimands. The main estimand of interest was the predicted values for the individual values of potassium over time.

Methods. For Scenario 1, we applied 10 different methods to the longitudinal potassium data to each simulated dataset. Five corresponds to the linear mixed model fitted with degrees of freedom for the spline transformation of time going from 5 to 9. The other five correspond to the mixed-wavelet approach, in which the linear mixed model is fitted with degrees of freedom for the splines going from 5 to 9. For Scenario 2, we applied both the MM and the mixed wavelet with a linear effect for time, a spline transformation of time with 4 and 5 degrees of freedom. The one with 5 degrees of freedom is the true data-generating model in Scenario 2.

Performance measure. The performance measure of interest in this part of the simulation study is a Mean Squared Error (MSE).

Results. The results are shown in Figure 1. In Scenario 1, the proposed approach based on the MW filter showed the highest performance in capturing the true individual biomarker profiles compared to the linear mixed model. Importantly, unlike the MM approach, MW appears to be more robust to the choice of the number of degrees of freedom used to account for the nonlinear effect of time. In Scenario 2, when the MM is correctly or nearly correctly specified, both the MM and WM capture the longitudinal biomarker profiles very well. This was an expected result for the MM, and it also showed that the MW filter works when it is not needed, as it simply returns zero short-term components. When we fit the MM and MW with a highly misspecified mixed model that assumes the linear longitudinal trajectories, the MSE increases for both methods; however, the MW performs best because it is most likely able to capture some of the nonlinear patterns that are missed by the MM.

4.2 | Dynamic Survival Predictions

Aims. In the second part of the simulation study, we aimed to assess the performance of the different landmark survival models in terms of dynamic predictive accuracy.

Data-generating mechanism. To generate the survival data, five different scenarios are considered:

- Under *Scenario 1.A*, it is assumed that the longitudinal potassium measures are from Scenario 1 described in Section 4.1, and it is assumed that the risk of death only depends on a smooth potassium component that follows a linear mixed-effect model similar to the one in Equation (2) with a spline transformation of time with 5 degrees of freedom.
- Under *Scenario 1.B*, it is assumed that the longitudinal potassium measures are from Scenario 1 described in Section 4.1, but the risk of death depends also on the short-term component as defined by the WM filter assuming that all durations between 2 and 365 days have the same prognostic value.
- *Scenario 1.C* is similar to Scenario 1.B but assumes that the short-term component obtained from the WM filter has different prognostic values depending on the duration intervals

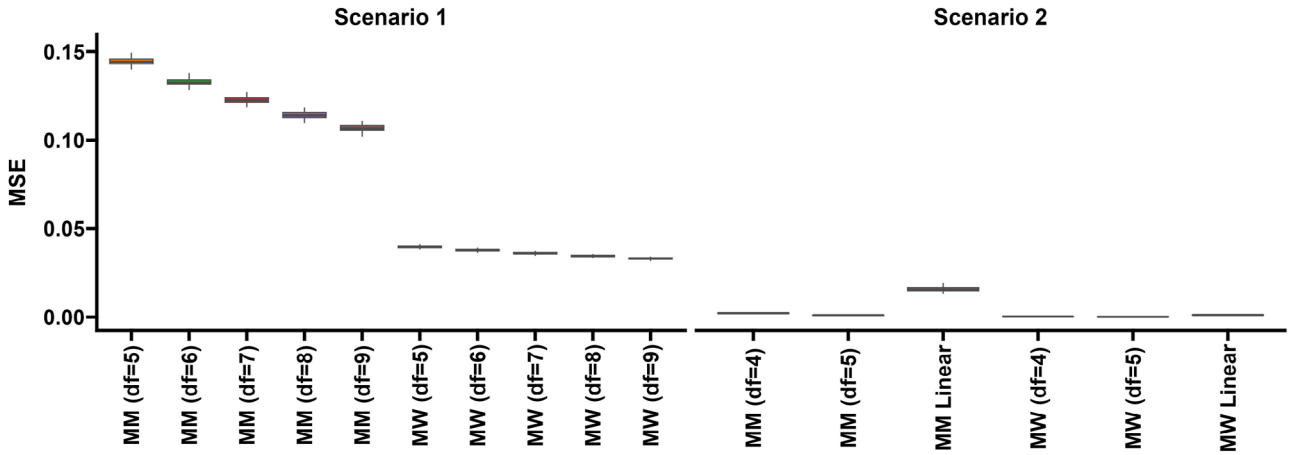

FIGURE 1 | Mean squared error (MSE) obtained in the simulation study for the mixed model (MM), and the Morlet wavelet–based method (MW).

which are 2–14 days, 15–30 days, 31–90 days, 91–180 days, and 181–365 days.

- *Scenario 1.D* is similar to Scenario 1.C but assumes that the short-term components obtained from the WM filter have the same prognostic values regardless of their amplitude.
- In *Scenario 2.A*, it is assumed that the longitudinal potassium measures are from Scenario 2 described in Section 4.1 and it is assumed that the risk of death only depends on the mean current value of potassium that follows a linear mixed-effect model similar to the one in Equation (2) with a spline transformation of time with 5 degrees of freedom.

The baseline hazard is assumed to follow a Weibull distribution and it depends on the landmark time, as in the models considered in Section 3.

Estimand. The estimand of interest was the predicted survival probability on a time horizon of 6 months at the landmark times considered are 1, 2, and 3 years.

Methods. We fitted different landmark survival models to each simulated survival landmark dataset:

- **LOCF**. The landmark model takes into account only the last observed biomarker.
- **MM (4 df)**.The mixed-landmark model where the MM for the biomarker is fitted with a spline with 4 degrees of freedom.
- **MM (5 df)**. The mixed-landmark model where the MM for the biomarker is fitted with a spline with 5 degrees of freedom.
- **MW a (4 df)**. The mixed-wavelet landmark model where the MM for the biomarker is fitted with a spline with 4 degrees of freedom and the $\hat{s}_i(h)^{2-365}$ is used as a short-term component.
- **MW a (5 df)**. The mixed-wavelet landmark model where the MM for the biomarker is fitted with a spline with 5 degrees of freedom and the $\hat{s}_i(h)^{2-365}$ is used as a short-term component.
- **MW b (4 df)**. The mixed-wavelet landmark model where the MM for the biomarker is fitted with a spline with 4 degrees of freedom, and the continuous version of the wavelet short-term components is used considering the intervals 2–14 days, 15–30 days, 31–90 days, 91–180 days, and 181–365 days.
- **MW b (5 df)**. The mixed-wavelet landmark model where the MM for the biomarker is fitted with a spline with 5 degrees of freedom, and the continuous version of the wavelet short-term components is used considering the intervals 2–14 days, 15–30 days, 31–90 days, 91–180 days, and 181–365 days.
- **MW c (4 df)**. The mixed-wavelet landmark model where the MM for the biomarker is fitted with a spline with 4 degrees of freedom, and the categorical version of the wavelet short-term components is used considering the intervals 2–14 days, 15–30 days, 31–90 days, 91–180 days, and 181–365 days.
- **MW c (5 df)**. The mixed-wavelet landmark model where the MM for the biomarker is fitted with a spline with 5 degrees of freedom, and the categorical version of the wavelet short-term components is used considering the intervals 2–14 days, 15–30 days, 31–90 days, 91–180 days, and 181–365 days.

Performance measure. The performance indices of interest were the dynamic Area Under the Curve (AUC(t)) and the Brier score. Tenfold cross-validation was used to obtain both indices. The prediction horizon considered was 6 months. For the definition of AUC(t) and the Brier score, the one proposed by Blanche et al. (2015) was used.

Results. The results are shown in Figure 2. In all scenarios, the LOCF is the model that performed worst. Under Scenario 1A, the MM (df = 5), which is the correctly specified model, MW a (df = 5), MW b (df = 4), MW b (df = 5), MW c (df = 4), and MW c (df = 5) all performed well. Both the MM (df = 4) and the MW a (df = 4) seem to suffer from the misspecification of the MM. Under Scenario 1B and Scenario 1C, the correctly specified models, MW a (df = 5) and MW b (df = 5), respectively, performed best. In Scenario 1C, MW b (df = 5) was followed by the other models that contained the short-term component divided by intervals. Under Scenario 1D, the correctly specified model, MW c (df = 5) performed best followed by the other MW models that considered the different short-term components. It can be observed that the specification of the MM component influences the discrimination. However, In Scenario 1B, it can be noticed that the discrimination of the mixed-wavelet

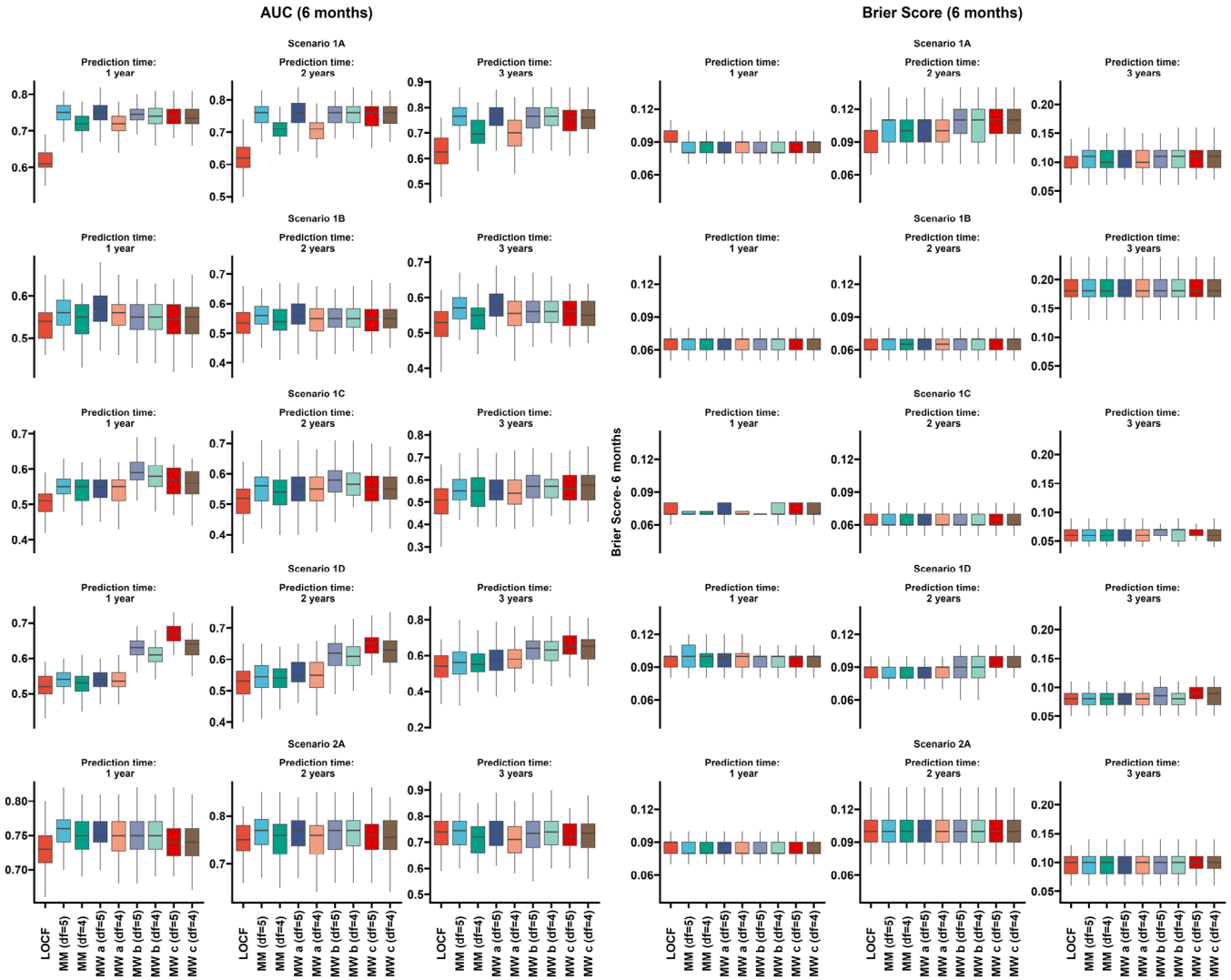

FIGURE 2 | AUC (6 months) and Brier score (6 months) obtained in the second part simulation study under the different scenarios and methods considered.

also suffers from the specification of the short-term component. Finally, under Scenario 2A, the correctly specified model had the best Area Under the Curve. It is also interesting to notice that the models MW a and MW b did not perform much worse, likely because the short-term components were not influential, similar to what was observed in the first part of the simulation study.

5 | Application

5.1 | Study Cohort

In total, 2981 subjects were included in the analysis. Their characteristics at the index date are summarized in Table 1. The median age in the cohort was 77 years (Interquartile Range: 70–83) and 58% were male. The median left ventricular ejection fraction (LVEF) was 54% (Interquartile Range: 40-63). LVEF is a measure of heart function, and it is considered to be normal when it is over 50%. In this cohort, 40% of patients had a reduced LVEF. The New York Heart Association (NYHA) class indicates the progression of heart failure. In this case, 88% of patients had a class of 1 or 2 corresponding to asymptomatic and mild symptoms, respectively. Furthermore, 48% of patients had a diagnosis of CKD and 64% of patients had more than 3 noncardiac comorbidities. The median time of the follow-up period in the cohort was 55 months (Interquartile Range: 33–80 months). Finally, subjects had a median number of potassium measurements of 20 (Interquartile Range 11–36) at a median distance of 4 days (IQR: 1–32 days). At 2 years of follow-up, the Kaplan–Meier estimate of the survival probability was equal to 0.92 (95%CI 0.91-9.93).

5.2 | Longitudinal Potassium Trajectories

To explore the relationship between the risk of death and potassium (K) in Figure 3, we show the trajectories of potassium observed for a random sample of 200 patients, considering the measurements before three possible landmark points. Patients have been divided into two groups: subjects who died in the 6 months following the landmark time and patients still alive at the end of the 6 months. After the first landmark time, eight

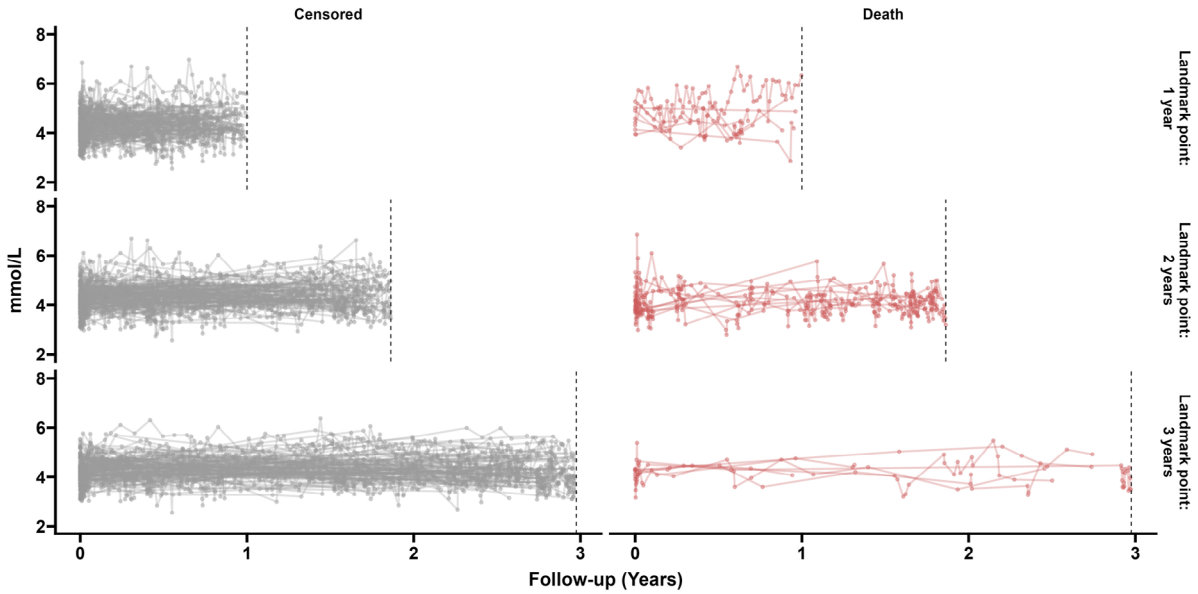

FIGURE 3 | Potassium measurements in a random sample of 200 patients before three possible landmark times dividing patients who die in the 6 months following the landmark point (red lines) from patients that are still alive after 6 months (black lines).

TABLE 1 | Descriptive statistics of the cohort. The median and the interquartile range is used to describe numerical variables and the absolute and relative frequency is used to describe categorical variables.

Variable	$n = 2981$
Age, years	77 (70, 83)
Gender, male	1730 (58%)
LVEF, %	54 (40, 63)
LVEF class	
HFpEF	1780 (60%)
HFrEF	1201 (40%)
NYHA Class	
I	1102 (37%)
II	1516 (51%)
III	337 (11%)
IV	26 (0.9%)
CKD	1422 (48%)
Non-cardiac comorbidities > 3	1915 (64%)
Number of potassium measurements	20 (11, 36)

patients died within 6 months. Out of the 175 patients still under observation after 2 years, 11 died within the following 6 months. After 3 years of follow-up, out of the 200 patients, 139 are still under observation and 7 are within 6 months from the third landmark point. It can be observed that the smoothed curve obtained through LOWESS falls within the standard normality range of 3.5–5 mmol/L in both groups. From the individual observed trajectories, it can be also observed some of the patients who died tend to exhibit an oscillatory pattern towards the end of the follow-up.

5.3 | Dynamic Survival Models

In all the landmark models presented in the following, as landmark points, we considered time points from 1 to 5 years at a distance of 7 days. The time horizon was fixed at 6 months. As fixed covariates, relevant prognostic factors in heart failure we considered: age, sex, NYHA class, LVEF class, diagnoses of CKD, and a burden of noncardiac comorbidities greater than three. For abbreviations, for potassium, the same notation used in the models presented in the Methods section will be used in the tables. Moreover, $ns(\cdot)$ will denote that a cubic B-spline was used as transformation $f(\cdot)$. All the results for the dynamic survival models considered are reported in Table 2. The models were fitted using the `R survival` package (Therneau and Grambsch 2000; Therneau 2022).

5.3.1 | Landmark LOCF

First, the two different landmark models, LOCF a and LOCF b were fitted to the data. Coherently with previous literature, all fixed covariates are risk factors, increasing the risk of death in heart failure patients. The last value of potassium as a continuous variable is also significant. Because of the spline transformation, its effect on the risk of death is shown in Figure 4. As expected, both high value and low value of potassium are associated with a greater hazard of dying in the next 6 months.

According to the results of the model LOCF b, having the last measurement of potassium below 3.5 mmol/L is associated with an increased risk of death, while having the last measurement of

TABLE 2 | Estimates of coefficients from the different landmark models along with standard errors, 95% confidence intervals, and, *p*-value.

LOCF a				
Variable	**Coefficient**	**Std. Error**	**95% CI**	***p*-value**
Age	0.68	0.05	0.58, 0.78	<0.01
Sex, male	0.31	0.07	0.16, 0.45	<0.01
NYHA III-IV (vs. I-II)	0.60	0.09	0.42, 0.77	<0.01
HFrEF	0.15	0.07	0.01, 0.29	0.04
>3 comorbidities	0.44	0.08	0.28, 0.59	<0.01
$ns_1(y_{ih})$	−4.37	0.57	−5.48, −3.26	<0.01
$ns_2(y_{ih})$	−3.01	0.54	−4.07, −1.96	<0.01
$ns_3(y_{ih})$	−4.54	1.26	−7, −2.07	<0.01
$ns_4(y_{ih})$	0.58	1.01	−1.4, 2.56	0.57
LOCF b				
Variable	**Coefficient**	**Std.Error**	**95% CI**	***p*-value**
Age	0.68	0.05	0.58, 0.78	<0.01
Sex, Male	0.31	0.07	0.17, 0.45	<0.01
NYHA III-IV (vs. I-II)	0.60	0.09	0.42, 0.77	<0.01
HFrEF	0.14	0.07	0, 0.29	0.05
>3 comorbidities	0.44	0.08	0.28, 0.59	<0.01
$y_{ih} > 5$ mmol/L	−0.02	0.09	−0.19, 0.15	0.83
$y_{ih} < 3.5$ mmol/L	0.89	0.12	0.65, 1.12	<0.01
MM				
Variable	**Coefficient**	**Std.Error**	**95% CI**	***p*−value**
Age	0.67	0.05	0.57, 0.77	<0.01
Sex, Male	0.31	0.07	0.17, 0.45	<0.01
NYHA III-IV (vs. I-II)	0.61	0.09	0.43, 0.78	<0.01
HFrEF	0.14	0.07	−0.01, 0.28	0.06
>3 comorbidities	0.43	0.08	0.28, 0.59	<0.01
$ns_1(\hat{m}_{ih})$	0.01	0.24	−0.46, 0.47	0.98
$ns_2(\hat{m}_{ih})$	0.09	0.15	−0.22, 0.39	0.58
$ns_3(\hat{m}_{ih})$	0.17	0.51	−0.82, 1.16	0.74
$ns_4(\hat{m}_{ih})$	0.02	0.27	−0.5, 0.54	0.93
$\hat{m}'_{ih}$	11.18	15.97	−20.11, 42.48	0.48
MW a				
Variable	**Coefficient**	**Std.Error**	**95% CI**	***p*-value**
Age	0.67	0.05	0.58, 0.77	<0.01
Sex, Male	0.31	0.07	0.17, 0.45	<0.01
NYHA III-IV (vs. I-II)	0.60	0.09	0.42, 0.78	<0.01
HFrEF	0.15	0.07	0.01, 0.29	0.04
>3 comorbidities	0.44	0.08	0.29, 0.6	<0.01
$ns_1(\hat{s}_{ih}^{[2-365]})$	−8.56	1.65	−11.8,−5.31	<0.01
$ns_2(\hat{s}_{ih}^{[2-365]})$	−3.37	1.16	−5.64, −1.1	<0.01
$ns_1(\hat{m}_{ih})$	−0.07	0.24	−0.54, 0.4	0.78
$ns_2(\hat{m}_{ih})$	−0.07	0.17	−0.4, 0.26	0.69
$ns_3(\hat{m}_{ih})$	−0.07	0.52	−1.08, 0.95	0.9
$ns_4(\hat{m}_{ih})$	−0.28	0.29	−0.84, 0.29	0.34

(Continues)

TABLE 2 | (Continued)

MW b				
Variable	**Coefficient**	**Std.Error**	**95% CI**	***p*-value**
Age	0.67	0.05	0.57, 0.77	<0.01
Sex, Male	0.30	0.07	0.15, 0.44	<0.01
NYHA III-IV (vs. I-II)	0.62	0.09	0.45, 0.8	<0.01
HFrEF	0.15	0.07	0.01, 0.29	0.03
>3 comorbidities	0.42	0.08	0.27, 0.57	<0.01
$ns_1(\hat{m}_{ih})$	−0.06	0.24	−0.52, 0.41	0.81
$ns_2(\hat{m}_{ih})$	0.08	0.16	−0.23, 0.38	0.63
$ns_3(\hat{m}_{ih})$	0.10	0.51	−0.9, 1.09	0.85
$ns_4(hatm_{ih})$	0.04	0.27	−0.48, 0.56	0.89
$\lvert\hat{s}_{ih}^{[2-14]}\rvert$	0.35	0.10	0.15, 0.54	<0.01
$\lvert\hat{s}_{ih}^{[15-30]}\rvert$	0.56	0.08	0.41, 0.72	<0.01
$\lvert\hat{s}_{ih}^{[31-90]}\rvert$	0.37	0.05	0.27, 0.47	<0.01
$\lvert\hat{s}_{ih}^{[91-180]}\rvert$	0.71	0.10	0.51, 0.9	<0.01
$\lvert\hat{s}_{ih}^{[181-365]}\rvert$	0.42	0.13	0.17, 0.67	<0.01
MW c				
Variable	**Coefficient**	**Std.Error**	**95% CI**	***p*-value**
Age	0.66	0.05	0.57, 0.76	<0.01
Sex, Male	0.29	0.07	0.15, 0.43	<0.01
NYHA III-IV (vs. I-II)	0.61	0.09	0.44, 0.78	<0.01
HFrEF	0.16	0.07	0.02, 0.3	0.03
>3 comorbidities	0.38	0.08	0.23, 0.54	<0.01
$ns_1(\hat{m}_{ih})$	0.05	0.24	−0.42, 0.52	0.82
$ns_2(\hat{m}_{ih})$	0.14	0.16	−0.16, 0.45	0.37
$ns_3(\hat{m}_{ih})$	0.24	0.51	−0.77, 1.25	0.64
$ns_4(\hat{m}_{ih})$	−0.05	0.26	−0.56, 0.47	0.86
$\hat{o}_{ih}^{[2-14]}$:upward	0.43	0.06	0.32, 0.55	<0.01
$\hat{o}_{ih}^{[2-14]}$:downward	0.45	0.05	0.34, 0.55	<0.01
$\hat{o}_{ih}^{[15-30]}$:upward	0.51	0.04	0.42, 0.59	<0.01
$\hat{o}_{ih}^{[15-30]}$:downward	0.49	0.04	0.41, 0.57	<0.01
$\hat{o}_{ih}^{[31-90]}$:upward	0.48	0.05	0.38, 0.58	<0.01
$\hat{o}_{ih}^{[31-90]}$:downward	0.50	0.05	0.4, 0.59	<0.01
$\hat{o}_{ih}^{[91-180]}$:upward	0.25	0.06	0.13, 0.37	<0.01
$\hat{o}_{ih}^{[91-180]}$:downward	0.30	0.06	0.19, 0.42	<0.01
$\hat{o}_{ih}^{[180-365-14]}$: upward	0.07	0.06	−0.05, 0.2	0.24
$\hat{o}_{ih}^{[180-365-14]}$: downward	0.13	0.06	0.01, 0.25	0.03

potassium greater than 5 mmol/L is not associated with a higher hazard of death.

5.3.2 | Mixed Landmark

The factors that are known to influence potassium are age, sex, CKD, and heart failure progression. For this reason, these variables, measured at baseline, were used as covariates in the linear mixed model for potassium. The estimates of the fixed coefficients show that males have a higher mean potassium value, CKD increases the mean potassium values, whereas an NYHA. A class above 2 is associated with lower potassium values.

The degrees of freedom for the spline transform of time were selected using the AIC. The model with a spline with 8 degrees of freedom was selected (Table 3).

The estimates for the fixed covariates are consistent with the results of the previous model. Moreover, as shown in panel B of Figure 4, the U-shape for the relative risk observed in the model LOCF is not evident anymore. A reason for this could be that the MM smooths the trajectory of potassium levels, which may result in values that are too stable to reflect the U-shape prognostic relationship. In contrast, the LOCF method in a very naive way captured more extreme values that come from short-term changes, making the relationship more evident.

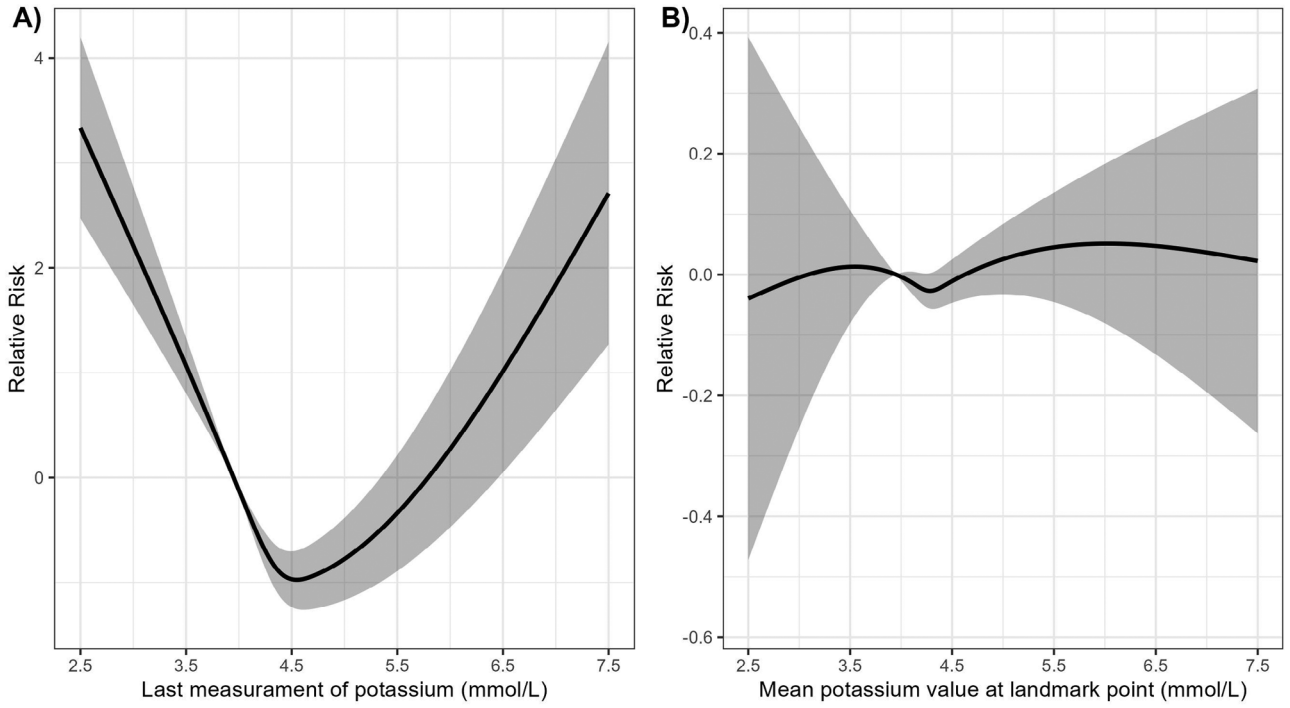

FIGURE 4 | Relative risk of the last value of potassium on the risk of death (panel A) and the mean value of potassium (panel B).

TABLE 3 | Estimates of the linear mixed effect model used for the MM and MW.

Variable	Coefficient	Std. Error	95% CI	*p*-value
Intercept	4.13	0.01	4.1; 4.15	<0.01
Sex, Male	0.06	0.01	0.04; 0.08	<0.01
Age	−0.00	0.01	−0.02; 0.01	0.43
CKD	0.12	0.01	0.1; 0.14	<0.01
NYHA III-IV (vs. I-II)	−0.06	0.02	−0.09; −0.02	<0.01
$ns_1(time)$	0.14	0.02	0.09; 0.18	<0.01
$ns_2(time)$	0.10	0.02	0.06; 0.15	<0.01
$ns_3(time)$	0.09	0.02	0.05; 0.13	<0.01
$ns_4(time)$	0.06	0.02	0.02; 0.1	<0.01
$ns_5(time)$	0.03	0.02	−0.01; 0.07	0.13
$ns_6(time)$	0.00	0.04	−0.08; 0.08	0.96
$ns_7(time)$	0.07	0.05	−0.04; 0.17	0.2
$ns_8(time)$	−0.17	0.11	−0.38; 0.05	0.13

5.3.3 | Landmark Mixed-Wavelet

Following the steps described in Section 3.4, we obtained the short-term component containing all changes of duration from 2 to 365 days, the vector of the continuous and categorical version of short-term changes differentiated between the different duration intervals. The MM used here was the same one used for the mixed landmark model (Table 3). Importantly, the procedure is repeated, considering all measurements of potassium before at each landmark point. As an example, the periodogram and the derived short-term oscillations together with the potassium measurements and the mean current value for one subject are presented in Figure 5.

Over the 5 years of observations, the mean trajectory estimated using the linear mixed effect model (top panel, dashed line) is rather flat. However, some sudden changes are captured by the periodogram (central panel). In correspondence to the stronger power spectrum areas, the filtering captures some changes in the interval 181–365 days and between 15 and 90 days.

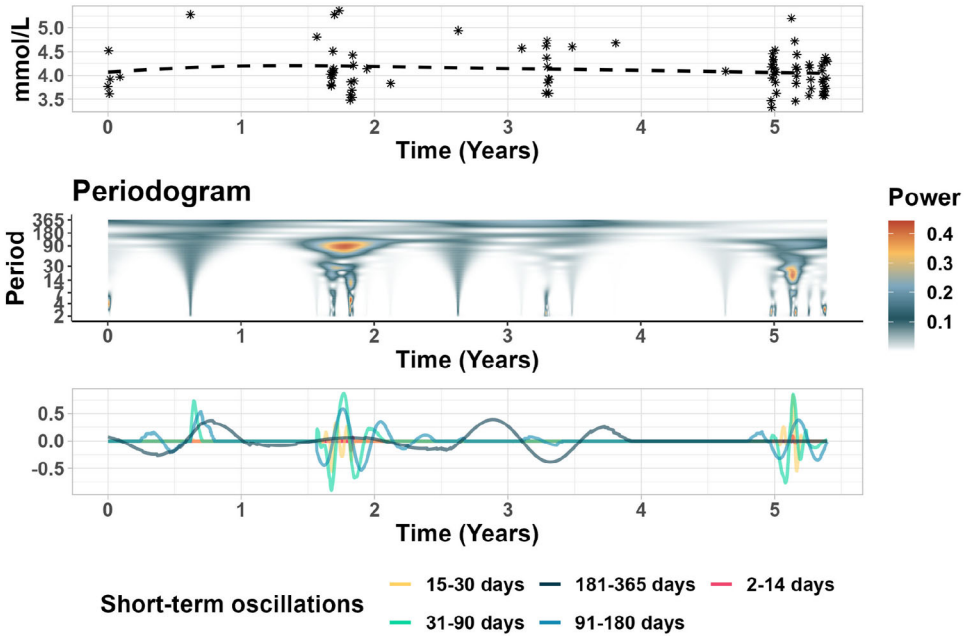

FIGURE 5 | Top panel: Potassium measurements over time and mean current value (dashed line) for one patient. Central panel: Periodogram obtained through the wavelet transform. Bottom panel: Example of corresponding short-term oscillations obtained through wavelet filtering.

As in the previous model, the mean value of potassium estimated through the linear mixed model does not appear to be significantly associated with the risk of death. In model MW a, the short-term component was modeled using a spline with 2 degrees of freedom, and the corresponding relative risk is reported in Figure 6. From this model, especially the downward overall changes between 2 and 365 days increase the risk of death. However, when we decompose the duration intervals in MW b and MW c, we observe that the presence of both downward and upward past variations in the last year has an impact on the risk of death with both downward and upward oscillations increasing the risk of death.

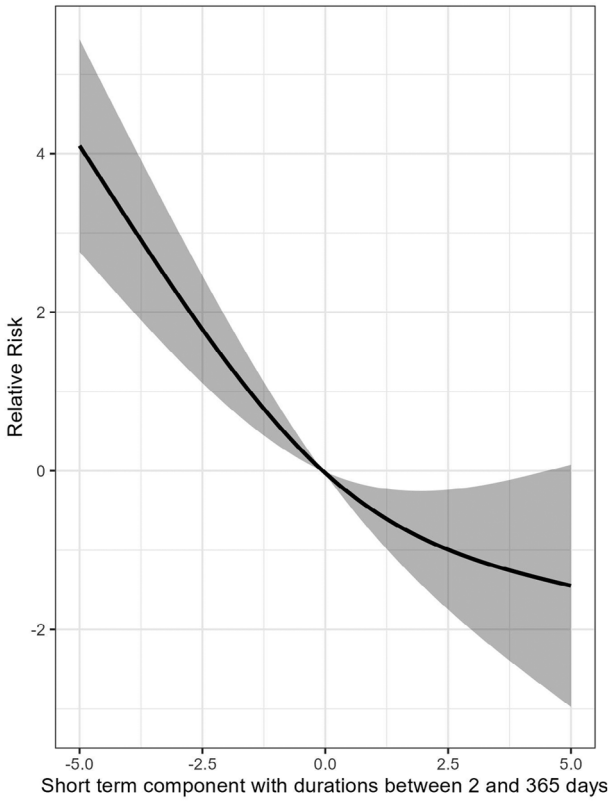

FIGURE 6 | Relative risk of the short-term component considered in model MW a.

5.4 | Models Comparison

First, the overall goodness-of-fit of the different landmark survival models was compared in terms of Aikake Information Criterion (AIC), Bayesian Information Criterion (BIC), and C-concordance index obtained with 10-fold cross-validation (Table 4). The landmark mixed-wavelet model shows the lowest AIC and BIC. Moreover, the C-index obtained with this approach is significantly higher than the others.

Similarly to the second part of the simulation study, a comparison of all the dynamic survival models in terms of the dynamic predictive performance was obtained through discrimination and calibration measures. Specifically, we used the AUC(t) and the Brier score. Tenfold cross-validation was used to obtain both indices. The prediction was made at three different times: 1 year, 2 years, and 3 years of follow-up, and the prediction horizon considered was 6 months. For the definition of AUC(t) and the Brier score, the one proposed by Blanche et al. (2015) was used. The results are presented in Table 5. It can be observed that the novel wavelet method showed the highest discrimination.

5.5 | Dynamic Predictions

In heart failure, the monitoring of potassium plays an important role. Therefore, a score that could easily be used by a cardiologist

TABLE 4 | Comparison of goodness-of-fit between the different landmark models in terms of AIC, BIC, and C-index (obtained with 10-fold cross-validation).

Model	AIC	BIC	C-Index (95% CI)
LOCF a	315,202	315,274	0.698 (0.683-0.714)
LOCF b	315,769	315,825	0.691 (0.674-0.709)
MM	316,378	316,458	0.685 (0.666-0.705)
MW a	316,240	316,328	0.69 (0.672-0.707)
MW b	314,361	314,473	0.708 (0.691-0.724)
MW c	311,361	311,512	0.73 (0.713-0.747)

TABLE 5 | Comparison of predictive accuracy measures between the different dynamic survival models in terms of discrimination and calibration (obtained with 10-fold cross-validation).

Prediction time: 1 year		
Model	**AUC (6 months)**	**Brier score (6 months)**
LOCF a	0.52 (0.46-0.57)	0.038 (0.032-0.045)
LOCF b	0.51 (0.47-0.55)	0.038 (0.032-0.045)
MM	0.57 (0.52-0.61)	0.038 (0.032-0.045)
MW a	0.59 (0.56-0.63)	0.038 (0.032-0.045)
MW b	0.65 (0.6-0.69)	0.038 (0.032-0.045)
MW c	0.67 (0.63-0.71)	0.038 (0.031-0.044)
Prediction time: 2 years		
Model	**AUC (6 months)**	**Brier score (6 months)**
LOCF a	0.61 (0.54-0.68)	0.041 (0.033-0.049)
LOCF b	0.53 (0.47-0.59)	0.041 (0.033-0.049)
MM	0.52 (0.46-0.58)	0.041 (0.033-0.049)
MW a	0.57 (0.5-0.63)	0.041 (0.033-0.049)
MW b	0.66 (0.59-0.73)	0.041 (0.033-0.049)
MW c	0.68 (0.6–0.75)	0.04 (0.032–0.048)
Prediction time: 3 years		
Model	**AUC (6 months)**	**Brier Score (6 months)**
LOCF a	0.52 (0.44-0.6)	0.05 (0.043-0.057)
LOCF b	0.51 (0.5-0.52)	0.051 (0.044-0.058)
MM	0.51 (0.47-0.55)	0.051 (0.044-0.058)
MW a	0.51 (0.47-0.56)	0.051 (0.044-0.058)
MW b	0.59 (0.55-0.64)	0.05 (0.043-0.058)
MW c	0.61 (0.56-0.66)	0.05 (0.043-0.057)

would be very useful to quantitatively assess the patient's risk using the potassium measurements available. Figure 7 shows an example of a patient's predicted survival probability dynamically updated at times 1.6, 2, and 3.3 years. In addition to the dynamic prediction of the survival probability, we also propose a score based on the wavelet landmark model, which feeds a dynamic tool for supporting medical doctor's daily practice. To obtain the score, the partial linear predictor, containing all the terms related to potassium, was predicted for an individual i at time t and it was categorized into risk groups by using the observed quartiles in the entire cohort. We call this the Heart Functional Dynamic Potassium (K) Score (HFDKS). Figure 7 also displays the corresponding predicted HFDKS. It can be observed how at one year and a half of follow-up, while having a previous potassium value over 5 mmol/L, the patient is at low risk. The risk becomes very high at 2 years after the subject has experienced multiple abrupt changes. At time 3.3 years of follow-up, the score decreases as changes have been less extreme. As expected, the predicted 6-month survival probability shows a similar pattern, with a lower probability of survival in the following 6 months at 2 and 3.3 years of follow-up.

6 | Discussion and Conclusions

In this paper, we tackled the problem of providing a suitable dynamic survival model to assist in the monitoring of potassium in heart failure patients using a landmark approach. In this disease, it is very important to monitor potassium since it is often altered by the disease as well as pharmacological treatments. The relationship between potassium and survival in heart failure remains debated, and the role of its dynamics over time has not been studied yet. Currently, in the clinical practice normality cutoffs on a single measurement are the only available quantitative method to assess patients' situation with regard to potassium. The extensive research carried out in the field of the dynamic survival model has shown the importance of exploiting the information provided by repeated measurements to take into account measurement error and past history of the biomarker process. Most of the dynamic survival models have focused on mixed-effects models. Joint models (Rizopoulos 2012) are also a very common approach to obtaining dynamic predictions. The main difference with the mixed landmark model is that the estimation is carried out on two different populations (Ferrer et al. 2019). When the biomarker, in this case, potassium, has important, but not lasting changes, the linear mixed model is not flexible enough to capture this local variation since the model assumes that the trajectory of the biomarker is smooth over time. Hence, short-term changes are essentially lost in the error term. In addition, these short-term changes do have not a common structure across subjects, instead, they vary across individuals both in terms of timing and duration.

The mixed landmark models are very flexible, and they allow considering different association structures between the biomarker and the risk of death. Sylvestre and Abrahamowicz (2009) and Wagner et al. (2021) consider the case in which the risk of death depends on a weighted cumulative biomarker value estimated with a linear-mixed model. On the other hand, landmark models based on location-scale MMs (Hedeker et al. 2008) could be useful for applications where the variance differs by subject characteristics or overtime. However, neither of these methods addresses the problem of detecting and using short-term oscillations. To overcome this problem, we have proposed a novel method that combines linear mixed-effect modeling coupled with a functional approach based on wavelet filters. The linear mixed model allows capturing the effect of baseline covariates and the subject-specific long-term profiles, while the functional approach on the

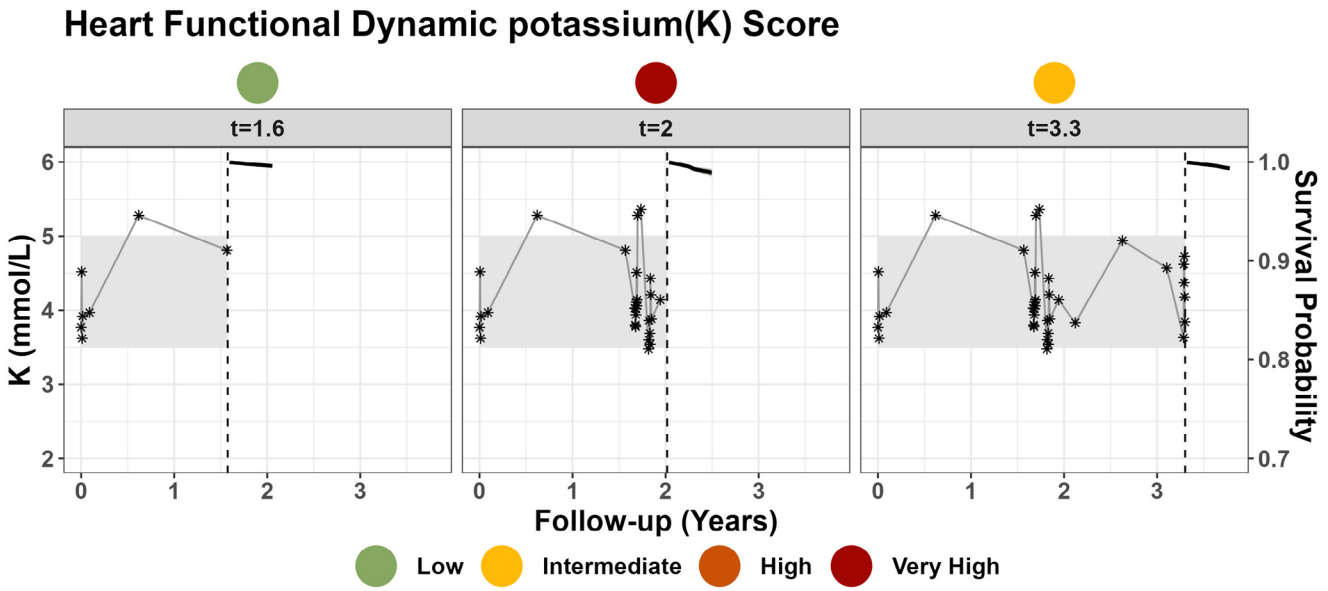

FIGURE 7 | Example of dynamic prediction for one patient's HFDKS and corresponding 6-month survival probability.

residuals allows identifying the individual short-term oscillations at different timings and of different durations. The simulation study showed that the choice of the number of degrees of freedom for the spline transform of time in the linear mixed model is less relevant when the mixed-wavelet approach is used compared to the classic MM. In addition, when the short-term changes are not present, the two models achieve similar performance. This was also true in the simulation study involving the survival landmark models. As expected, the dynamic predictive accuracy of the mixed-wavelet outperforms the mixed landmark model if the short-term biomarker changes affect the risk of death and if the association structure is specified appropriately. It is important to notice that if the short-term biomarker changes affect the risk of death but do not affect the survival or the short-term changes are not present in the biomarkers, the two approaches show a similar performance.

In addition, the proposed method enabled us to show the prognostic role of short-term changes in potassium, independently of the effect of the mean value of potassium. Thus, we laid the basis for a dynamic score to quantitatively summarize the risk of death associated with the observed history of potassium measurements. This is an important point since the goal of this work was also to provide a possible solution for the problem of monitoring potassium in clinical practice. In the context of the application presented, we compared the performance in terms of goodness-of-fit and dynamic predictive ability of our method with standard landmarking and the mixed-landmark model. The reason is that the smooth component of individual potassium trajectories is not the only relevant part of the longitudinal process from a prognostic point of view. On the contrary, the wavelet approach recovers the short-term oscillations and improves the performance of the survival model.

We believe that it would be of interest to study it further in other clinical settings involving long-term monitoring of biomarkers. Moments of crises in biomarkers translating into short-term changes can be quite common in chronic diseases, and our approach can help to study their role in a time-to-event setting. Specifically, the method is flexible in the definition of what short-term means. Both the choice of the maximum period to consider for the short-term oscillation and the intervals for the dimensionality reduction of the periodogram concerning the frequency domain can be chosen according to biological knowledge and sample size considerations. Importantly, the specification of the short-term component should be assessed through model diagnostics and predictive accuracy measures as the simulation study revealed that the method is sensible to such choices, similar to the mixed-landmark model. Given the sample size of the longitudinal data, the uncertainty propagated through the multistage estimation procedures of the mixed and mixed-wavelet models was found to be negligible. However, a nested parametric bootstrap method could be employed if different data or markers are used and this is not the case when calculating the standard error of the MM and MW models. In conclusion, in studying the relationship between potassium and survival, the most important aspect consists of modeling the dependence of the survival process on the biomarker's past. In our work, we were able to explore how much of the history of the potassium process is relevant to the time-to-event process.

At the moment, the linear mixed model component and the short-term components are estimated in two steps. In the future, it could be of interest to develop a method to obtain them simultaneously. Moreover, we are aware that the landmark model is a working model, and it would be more satisfactory and coherent from a statistical perspective to introduce a joint model that includes the wavelets in the longitudinal component. However, it would also be far more challenging from a computational point of view, especially given the amount of data present in studies involving electronic health records. We believe that this work and the promising results obtained in this application with the wavelet landmark prove that it is worth it to keep working in this direction and that there is still space for improvement in the field of dynamic survival models. In the future, it could be of interest to externally validate the method considering the same applications

or different clinical problems. An essential future step to allow for such a method to be applied in clinical practice consists of obtaining the confidence intervals for the dynamic predictions that take into account the multistep procedure involved in the mixed and mixed-wavelet landmark model.

Acknowledgments

This work was supported by VIFOR Pharma. The authors also thank Dr.Annamaria Iorio for her cardiological insights.

Conflicts of Interest

The authors declare no conflicts of interest.

Data Availability Statement

The real-data that support the findings of this study is not available for ethical and privacy reasons. Realistic synthetic data is available in the Supporting Information section.

Open Research Badges

This article has earned an Open Data badge for making publicly available the digitally-shareable data necessary to reproduce the reported results. The data is available in the Supporting Information section.

This article has earned an open data badge "**Reproducible Research**" for making publicly available the code necessary to reproduce the reported results. The results reported in this article were reproduced partially due to data confidentiality issues.

References

Blanche, P., C. Proust-Lima, L. Loubère, C. Berr, J. F. Dartigues, and H. Jacqmin-Gadda. 2015. "Quantifying and Comparing Dynamic Predictive Accuracy of Joint Models for Longitudinal Marker and Time-to-Event in Presence of Censoring and Competing Risks." *Biometrics* 71, no. 1: 102–113.

Carmona, R., W.-L. Hwang, and B. Torresani. 1998. *Gabor and Wavelet Transforms With an Implementation in S*. 1st ed. Academic Press.

Cooper, L. B., L. Benson, R. J. Mentz, et al. 2020. "Association Between Potassium Level and Outcomes in Heart Failure With Reduced Ejection Fraction: A Cohort Study From the Swedish Heart Failure Registry." *European Journal of Heart Failure* 22, no. 8: 1390–1398.

Ferreira, J. P., J. Butler, P. Rossignol, et al. 2020. "Abnormalities of Potassium in Heart Failure: JACC State-of-the-Art Review." *Journal of the American College of Cardiology* 75, no. 22: 2836–2850.

Ferrer, L., H. Putter, and C. Proust-Lima. 2019. "Individual Dynamic Predictions Using Landmarking and Joint Modelling: Validation of Estimators and Robustness Assessment." *Statistical Methods in Medical Research* 28, no. 12: 3649–3666.

Hedeker, D., R. J. Mermelstein, and H. Demirtas. 2008. "An Application of a Mixed-Effects Location Scale Model for Analysis of Ecological Momentary Assessment (EMA) Data." *Biometrics* 64, no. 2: 627–634.

Iorio, A., G. Sinagra, and A. Di Lenarda. 2019. "Administrative Database, Observational Research and the Tower of Babel." *International Journal of Cardiology* 284: 118–119.

Morris, T. P., I. R. White, and M. J. Crowther. 2019. "Using Simulation Studies to Evaluate Statistical Methods." *Statistics in Medicine* 38, no. 11: 2074–2102.

Nason, G. P., and R. Von Sachs. 1999. "Wavelets in Time-Series Analysis." *Philosophical Transactions of the Royal Society of London. Series A: Mathematical, Physical and Engineering Sciences* 357, no. 1760: 2511–2526.

Rizopoulos, D. 2012. Joint Models for Longitudinal and Time-to-Event Data: With Applications in R, 1–257. Routledge.

Rizopoulos, D., G. Molenberghs, and E. M. Lesaffre. 2017. "Dynamic Predictions With Time-Dependent Covariates in Survival Analysis Using Joint Modeling and Landmarking." *Biometrical Journal* 59, no. 6: 1261–1276.

Rösch, A., H. Schmidbauer, A. Roesch, and H. Schmidbauer. 2018. "WaveletComp: Computational Wavelet Analysis." https://cran.r-project.org/package=WaveletComp.

Sylvestre, M.-P., and M. Abrahamowicz. 2009. "Flexible Modeling of the Cumulative Effects of Time-Dependent Exposures on the Hazard." *Statistics in Medicine* 28, no. 27: 3437–3453.

Therneau, T. M., and P. M. Grambsch. 2000. *Modeling Survival Data: Extending the Cox Model*. Springer.

Therneau, T. M. 2022. "A Package for Survival Analysis in R." https://cran.r-project.org/package=survival.

Unser, M., and A. Aldroubi. 1996. "A Review of Wavelets in Biomedical Applications." *Proceedings of the IEEE* 84, no. 4: 626–638.

van Houwelingen, H. C., and H. Putter. 2011. *Dynamic Prediction in Clinical Survival Analysis*. CRC Press.

Wagner, M., F. Grodstein, K. Leffondre, C. Samieri, and C. Proust-Lima. 2021. "Time-Varying Associations Between an Exposure History and a Subsequent Health Outcome: A Landmark Approach to Identify Critical Windows." *BMC Medical Research Methodology* 21, no. 1: 266.

Supporting Information

Additional supporting information can be found online in the Supporting Information section.